AAS 11-543

OPTIMAL CONSTELLATION DESIGN FOR SPACE BASED SITUATIONAL AWARENESS APPLICATIONS

A.T. Takano* **and B.G. Marchand†**

Modern space situational awareness is focused on the detection, tracking, identification, and characterization of passive and active resident space objects. In the past, this process relied primarily on ground-based sensors. However, difficulties arise when smaller objects are considered, in the nano- or pico-satellite range for instance. To supplement ground sensing capabilities, a constellation of space based sensors is envisioned. In this study, concepts from computer graphics and numerical optimization are fused into a unique constellation design approach for space based space situational awareness applications.

INTRODUCTION

As near-Earth space becomes increasingly crowded with spacecraft and debris, the need for improved space situational awareness (SSA) has become paramount. Modern SSA is concerned with the detection, tracking, identification, and characterization (DTI&C) of passive and active resident space objects (RSOs), at all altitudes, with known accuracy and precision. RSOs are said to be active if they are capable of maneuvering, and passive if they are not.

Modern advances in technology miniaturization, and the growing capabilities of nano- and pico-satellite platforms, have raised many new and exciting technical challenges in this area. Contemporary ground-based systems, such as the space surveillance network (SSN), are often unable to identify objects in the pico-satellite range, much less characterize the active RSOs functionality or predict its path or attitude with sufficient accuracy.

A new area of study focuses on space based space situational awareness (SBSSA) to provide DTI&C in lieu of, or in conjunction with existing ground-based systems. In this study SBSSA goals are accomplished through a network of space based sensors, i.e. a constellation of satellite sensing platforms. Although these sensors are devoted to the DTI&C of the same RSOs ground-based systems are concerned with, their operational environment is significantly different. The necessary nature of the sensors on each platform, and their optimal arrangements and orientations, will then depend on the specific DTI&C goals that are of interest in a given circumstance. Techniques for analysis and optimal design of a network of space-based sensors that adequately supplements DTI&C goals are the focus of the present investigation.

The constellations providing ATH coverage as a primary objective are quite different from those previously considered.[1–3] Traditionally, constellation design is focused on providing ground cov-

*Graduate Student, Department of Aerospace Engineering, The University of Texas at Austin, 210 E. 24th St., Austin, TX 78712. Email: andrewtakano@utexas.edu

†Assistant Professor, Department of Aerospace Engineering, The University of Texas at Austin, 210 E. 24th St., Austin, TX 78712. Email: marchand@alumni.purdue.edu

erage, or coverage below the horizon (BTH) from the perspective of each satellite (i.e. coverage of targets against an Earth background). In contrast, the present study considers coverage above the horizon (ATH), where satellite sensors scan for RSOs against a space background.[4–6] This approach enables use of sensors with significant improvements in dim target detection compared to ground-based systems.[7]

In the current study the 'horizon' is defined relative to a prescribed tangent height above the Earth's limb that is used to define the Earth-centered tangent height shell (THS), as indicated in Figure 1. The tangent height is defined as the closest distance to the Earth's limb where a satellite's sensor is still able to observe objects in space.[4] ATH and BTH coverage regions are separated by an imaginary cone that emanates from the satellite and runs tangent to the horizon, enveloping the Earth and extending to infinity. This boundary is referred to as the tangent height cone (THC).[4] The in-plane cross-section of the THC, referred to as the tangent height triangle (THT) is shown in Figure 1.

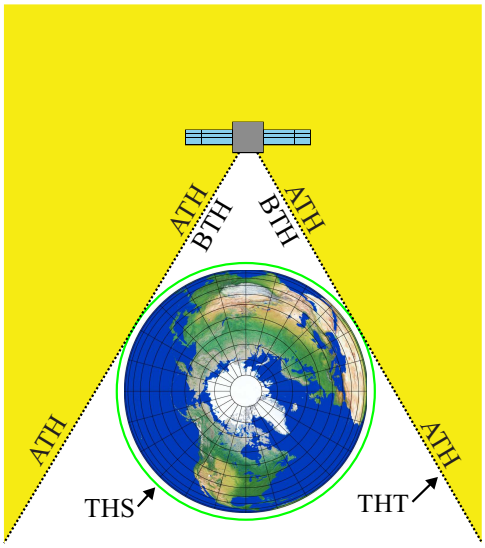

Figure 1: ATH vs. BTH Regions – In-Plane Cross-Section

Traditional Constellation Design Methods for ATH Coverage

ATH constellation design methods in the literature may be divided into two categories depending on the characterization of the target region – single-altitude and dual-altitude band regions. Analyses of single-altitude band target regions[5,7–9] only consider the region between the THS and an upper target altitude shell (UTAS). Dual-altitude band target regions[4,6] expand upon this by defining an arbitrary lower target altitude shell (LTAS) that is above the THS and below the UTAS. These scenarios lead to coverage regions of fundamentally different shapes. Typical coverage regions within single- and dual-altitude band target regions are shown in Figure 2.

Multiple investigators[5,7–9] have published work concerning ATH coverage within the single-altitude band target region. Early analyses[8] only considered ATH coverage as a secondary objective to BTH coverage, and the techniques described there do not lend themselves to designing constellations specifically intended to provide ATH coverage. Rider[5] directly approaches the ATH

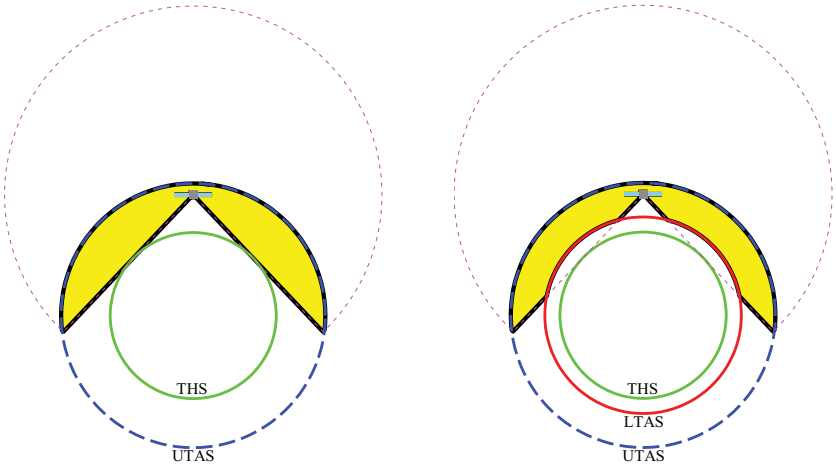

(a) Single-Altitude Band (b) Dual-Altitude Band

Figure 2: Examples of Single- and Dual-Altitude Band Coverage Regions

coverage problem for a single-altitude band target region analytically, using geometric reasoning to obtain solutions. The method constructed is analogous to the streets of coverage approach to the BTH coverage problem, dictating satellite positioning to ensure total ATH coverage. While his methods determine the necessary quantity and positioning of satellites to achieve coverage, they do not consider the actual amount of coverage in cases where the desired coverage is not achieved. Additionally, sensor range in Rider's study is considered to be unbounded. The necessary mass of a sensor or antenna may be approximated as increasing proportionally with the square of the desired effective range,[7] thus the simplifying assumption of unbounded sensor range is impractical.

Single-altitude band analyses may be considered a subset of the dual-altitude band coverage problem. The methods presented in the current study are equally applicable to single-altitude band, dual-altitude band, and arbitrary target regions of any planar form.

An early treatment of ATH coverage of a dual-altitude band target region is presented by Rider[6] who expands upon his earlier work on the single-altitude band ATH coverage problem to consider a prescribed lower altitude bound above the tangent height. The analysis considers various combinations of equatorial and polar orbital planes, again using geometric reasoning to obtain solutions.

More recent research, presented by Marchand and Kobel,[4] presents an analytical coverage model to explicitly evaluate in-plane ATH coverage area for the dual-altitude band coverage problem. In-plane coverage area provided by a single satellite with omni-directional sensors in a circular orbit is considered, leading to a time-invariant problem when the quantity of coverage area alone is of interest. However, coverage in a fully populated constellation may create regions of overlap where higher coverage multiplicities exist (i.e. regions that are simultaneously observed by multiple satellites). Consequently, the coverage provided by a single satellite does not scale intuitively to the total coverage of an entire constellation of similarly positioned and equipped satellites.

The primary difference between Marchand and Kobel's[4] result and earlier ATH coverage analyses[5–9] is that a measure of actual coverage is obtained. Previous analyses use methods to design constellations that by their very nature ensure the desired coverage characteristics. A model to compute the actual coverage, given a set of parameters, allows for constellation design optimization in a

different sense. Perhaps most importantly, it enables design using a variety of existing generalized numerical optimization methods.

General Approach

The numerical ATH coverage model developed and demonstrated in this study is presently only implemented for planar analysis. Thus, all satellites in a constellation under consideration must lie in a single orbital plane, and their sensor regions are assumed to exhibit some form of cross-plane symmetry such that in-plane coverage area correlates to three-dimensional coverage volume in some reasonable sense. At its most fundamental level, the model is simply a specific sequence of Boolean operations between the sensor coverage and target regions. Although a planar implementation using the polygon clipping technique[10–12] is used to perform the Boolean operations between polygons representing the relevant planar regions, the same sequences of operations may be directly applied to the volumetric case. Such an implementation would require incorporation of an algorithm to handle the Boolean operations between non-convex polyhedron.

The numerical nature of the model and implementation allow it to address, with greater ease to the investigator, more complex problems than previously developed analytical models.[4] Certainly, exact representations of the ATH coverage area are only available under a simplified set of assumptions. Even then, the process of identifying these analytical representations leads to highly complex non-unique piecewise differentiable coverage area functions. The numerical approach proposed in this investigation, while computationally more expensive, is applicable to any sensor profile and target region geometry, provided they can be approximated as polygons. Furthermore, the coverage within the target region can be determined for any desired coverage multiplicity, given a fully defined constellation. As discussed in the Application section, this numerical approach is particularly useful in SBSSA applications for constellation design, perhaps most readily to define coverage constraints or objectives in a parameter optimization problem.

METHODOLOGY

In this section a numerical model for the evaluation of ATH coverage provided by a constellation of sensors is developed. To demonstrate the general concept behind the methodology, without incurring large computational penalties, the analysis presented is planar. That is, all satellites are assumed to exist on the same orbital plane. Furthermore, although the sensor profiles are three-dimensional, as is the ATH target region, the coverage volume is not explicitly computed. Rather, the cross-sectional area of coverage - within the constellations orbit plane - is determined instead. The computation of the resulting 2-D ATH coverage area is accomplished through a specific sequence of Boolean operations between polygons that represent cross-sections of sensor profiles and target regions. These Boolean operations return both the coverage area and the coverage multiplicity. Boolean operations between polygons are performed using the well-established technique of polygon clipping,[10] traditionally used in digital image synthesis and geospatial information systems. This approach is used to evaluate ATH coverage of any desired multiplicity provided by planar constellations of any size. From a numerical perspective, the methodology presented is independent of the geometry of the sensor profile and target regions. However, cross-orbit-plane symmetry is required in order to maintain some correlation between the planar and volumetric coverage scenarios, i.e. as in-plane coverage area increases, so must coverage volume, and vice versa. Figure 3 illustrates ATH coverage of an Earth-centered annular target region provided by a planar constellation of sensor platforms with arbitrarily defined sensor profiles.

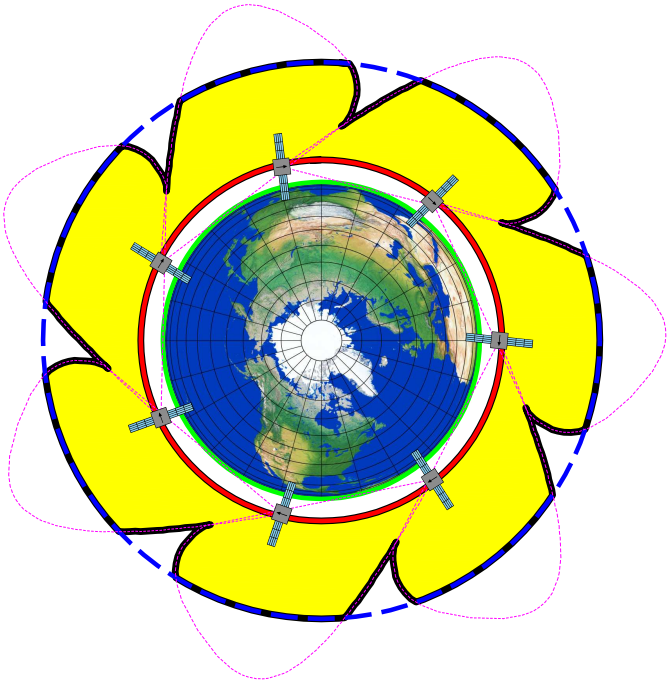

Figure 3: A Constellation of Platforms With Arbitrary Sensor Profiles Providing ATH Coverage

Defining Sensor Regions

Because the sensor profile of each satellite, and the target region are all represented as polygons, the number of points used to define each polygon will affect the accuracy of the coverage area calculations. The 'resolution' of a polygon, then, refers to the number of points per contour (PPC) that define its boundary. Polygons may have multiple contours (i.e. a region with an interior hole, or a polygon composed of multiple separate regions), thus, this variable indicates the number of vertices used to define each contour upon generation of the initial polygon.

Omni-Directional Sensor Regions For simplicity, much of the discussion in this study assumes omni-directional satellite sensors with no loss of generality. Under this assumption, the effective range shell (RS_E, the *actual* ATH region covered by the satellite, i.e. the sensor region excluding the BTH region) is computed by simple geometry. A notated illustration of the effective range shell is shown in Figure 4. The interior half angle of the THT, γ, is computed as

$$\gamma = \arcsin \frac{r_t}{r_s}. \tag{1}$$

Given an in-plane longitude (angular displacement of the satellite from the positive x-axis) of θ, it is then clear that the initial and final angles for the circular portion of the boundary are given by

$$\psi_i = \pi - \gamma + \theta, \tag{2}$$

$$\psi_f = -\pi + \gamma + \theta. \tag{3}$$

For a polygon resolution of m PPC, the first vertex lies at the satellite. The remaining $m - 1$ vertices are distributed along the outside circular arc of the sensor region, between angles ψ_i and

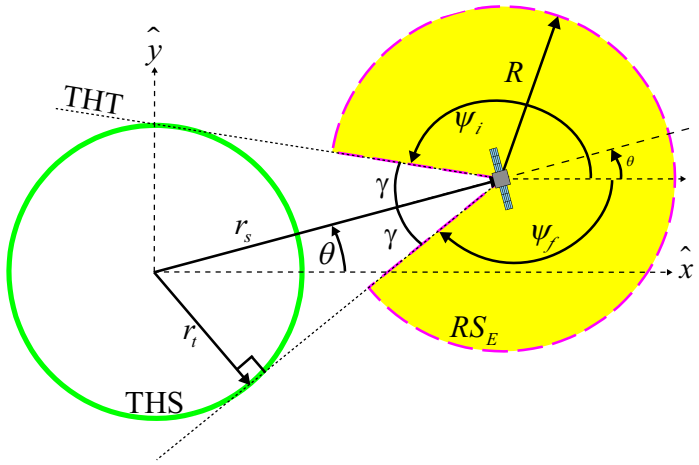

Figure 4: Notation for Computing Effective Range Shell (RS_E) Vertices for the Omni-Directional Sensor Case

ψ_f at radius R in a counter-clockwise direction. The curve is implicitly closed between the initial and final vertices.

Arbitrary Sensor Regions In analyzing non-omni-directional sensor regions with a known in-plane cross-section, the effective range shell, RS_E is isolated by subtracting the THT from the sensor region (by Boolean difference operation, using polygon clipping). Referring to Figure 5a, a polygon is defined representing the in-plane cross-section of the arbitrary sensor profile, RS_{arb} and the tangent height triangle, THT (Figure 5b). Although the THT extends to infinity, for practical purposes it need only extend beyond the sensor cross-section for this step. Because of the non-omni-directional shape, the in-plane attitude of the sensor cross-section must be considered, and the resulting effective range shell shape varies considerably with attitude, as shown in Figures 5c-5d. The additional clipping operation to isolate RS_E incurs a small performance penalty over the omni-directional case, where none is required. However, due to the low resolution of the THT, the performance penalty is typically negligible.[13]

Numerical ATH Coverage Model

For simplicity, the model development discussion considers omni-directional sensor platforms equally distributed in a single circular orbit. However, it is fundamental to observe that the same models apply to *any* configuration of satellites subject to the planar analysis this study is concerned with.

Single Multiplicity The basis for the single coverage model is illustrated in Figure 6. Here, $n-1$ union operations (Figures 6a-6i) are performed between the n satellite effective range shells, RS_E to produce a total effective sensor region, RS_{TE}. A final intersection operation with the target region, AS, yields the region of total single coverage within the target region, shown in Figure 6l as

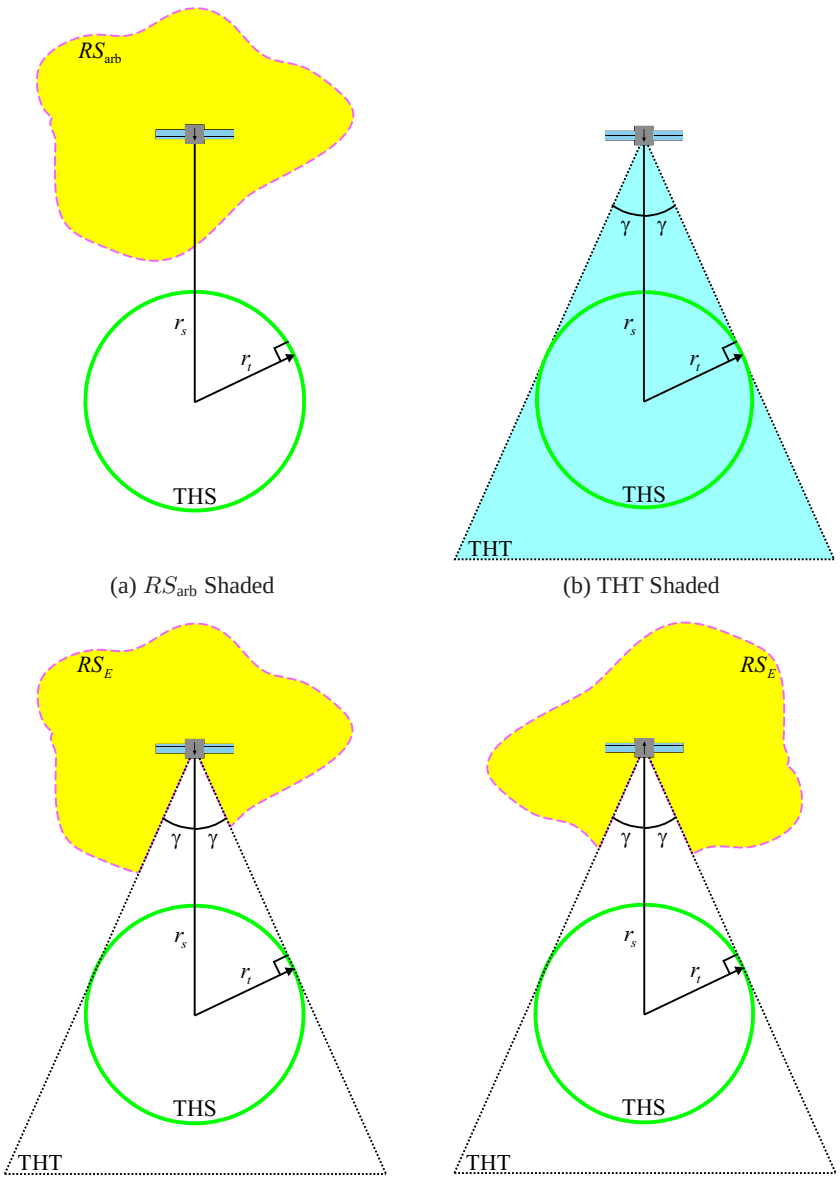

(a) RS_{arb} Shaded (b) THT Shaded

(c) 0° From Nadir Direction (d) 180° From Nadir Direction

Figure 5: RS_{arb} and THT: THT is Subtracted From RS_{arb} to Form RS_E

$C_{1\times}$, defined in set notation as

$$C_{1\times} = \left(\bigcup_{i=1}^{n} RS_{E_i} \right) \cap AS. \tag{4}$$

Determination of the area enclosed by $C_{1\times}$ is computed directly from the vertices of each polygon contour.[14] This method is applied to each contour of the resulting polygon $C_{1\times}$, adding areas inside fill regions to the total area, and subtracting areas inside hole regions.

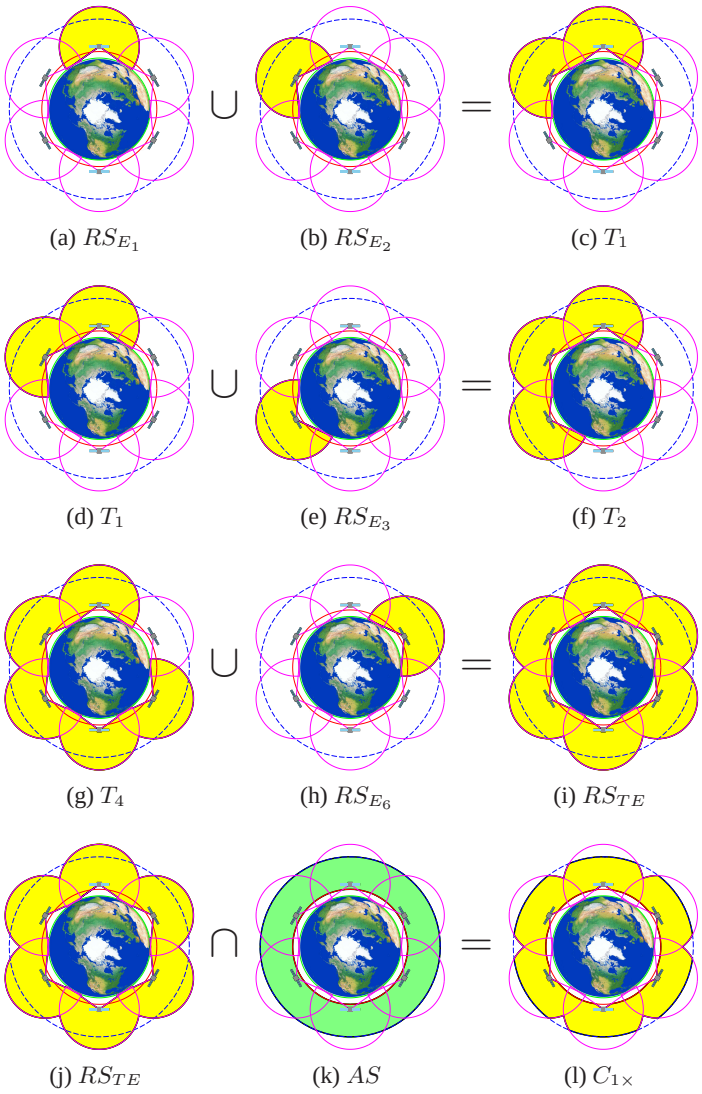

(a) RS_{E_1} (b) RS_{E_2} (c) T_1

(d) T_1 (e) RS_{E_3} (f) T_2

(g) T_4 (h) RS_{E_6} (i) RS_{TE}

(j) RS_{TE} (k) AS (l) $C_{1\times}$

Figure 6: Single Coverage Illustration – 6 Satellite Constellation

Double Multiplicity Determining regions of double coverage requires a different sequence of Boolean operations, as illustrated in Figure 7. Intersections between all unique pairs of sensor regions, as shown in Figures 7a-7f, isolate all regions of double sensor overlap. These regions are then combined using union operations (Figures 7g-7j). Finally, an intersection with the target region, yields $C_{2\times}$ (the region of double coverage within the target region), shown in 7l. This sequence is

expressed in set notation as

$$C_{2\times} = \left(\bigcup_{i_1=1}^{n-1} \bigcup_{i_2=i_1+1}^{n} \left(RS_{E_{i_1}} \cap RS_{E_{i_2}} \right) \right) \cap AS. \tag{5}$$

The indices for the union operations are chosen to avoid redundant or meaningless calculations, i.e. only address each unique combination of satellites once. For instance, performing $RS_{E_1} \cap RS_{E_2}$ followed by $RS_{E_2} \cap RS_{E_1}$ is a redundancy (they represent the same region – the intersection operator is commutative). Similarly, considering $RS_{E_1} \cap RS_{E_1}$ for double coverage is meaningless – RS_{E_1} cannot cover the same region twice. The area inside $C_{2\times}$ is evaluated just as in the single multiplicity case.

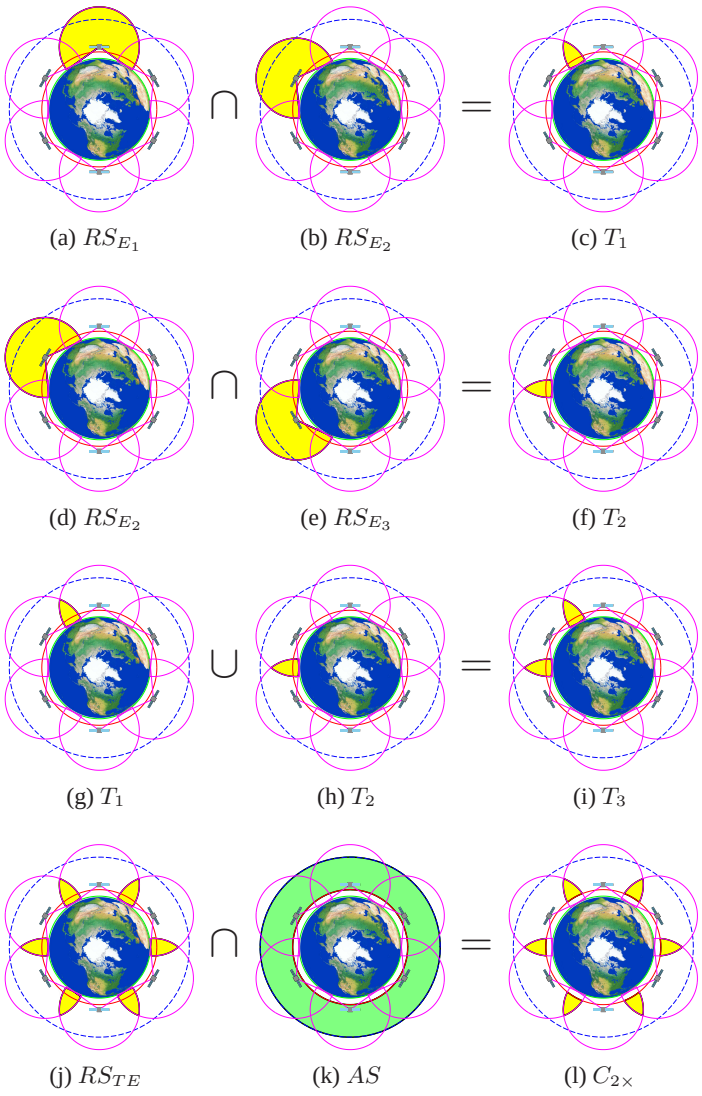

(a) RS_{E_1} (b) RS_{E_2} (c) T_1

(d) RS_{E_2} (e) RS_{E_3} (f) T_2

(g) T_1 (h) T_2 (i) T_3

(j) RS_{TE} (k) AS (l) $C_{2\times}$

Figure 7: Double Coverage Illustration – 6 Satellite Constellation

Arbitrary Multiplicity Upon performing a similar analysis to the triple multiplicity case,[13] a clear pattern emerges, yielding a general expression for p multiplicity coverage of an n satellite constellation, $C_{p\times}$:

$$C_{p\times} = \left(\bigcup_{i_1=1}^{n-p+1} \bigcup_{i_2=i_1+1}^{n-p+2} \cdots \bigcup_{i_{p-1}=i_{p-2}+1}^{n-1} \bigcup_{i_p=i_{p-1}+1}^{n} \left(RS_{E_{i_1}} \cap RS_{E_{i_2}} \cap \cdots \cap RS_{E_{i_p}} \right) \right) \cap AS. \quad (6)$$

Note that $n \geq p$. This is clear when considering the opposite case by logic alone – i.e., it is impossible for a three satellite constellation to yield quadruple coverage. This expression reduces to $C_{1\times}$and $C_{2\times}$for p values of 1 and 2 respectively. The enclosed area of $C_{p\times}$ is evaluated just as in the single multiplicity case.

Number of Clipping Operations

The performance of the numerical coverage model depends on polygon resolution, and the number of necessary clipping operations. Polygon resolution is chosen by the investigator based on the level of precision desired, while the number of satellites and the coverage multiplicity of interest dictate the number of clipping operations. The bounds on the finite unions in Equation (6) ensure consideration of all unique p-combinations from n satellites. Thus, $q_p(n) \equiv \binom{n}{p}$ is the number of possible p-combinations out of n satellites, and is determined by $n!/p!(n-p)!$.[15]

In general, $q_p(n)$ p-tuplets are each subject to $p-1$ intersections. The resulting $q_p(n)$ regions are combined by $q_p(n)-1$ unions, followed by one intersection with the target region, forming $C_{p\times}$. The total number of clip operations is $(p-1)q_p(n) + q_p(n) - 1 + 1$, or

$$Q_p(n) \equiv pq_p(n) = p\binom{n}{p} = \frac{n!}{(p-1)!(n-p)!}. \quad (7)$$

A plot of $Q_p(n)$ is shown in Figure 8. Although single coverage requires only n clipping operations, higher coverage multiplicities require a significantly larger number of clipping operations. For instance, for $n = 15$, up to 15 or 210 clip operations may be required to determine regions of single or double coverage, respectively. In contrast, for octuple coverage, up to 51,480 clip operations may be necessary, creating a highly computationally intensive problem.

Fortunately, $Q_p(n)$ is only an upper bound on the number of clip operations that will almost never occur in a practical implementation. While performing the intersections for a single p-tuplet, the program will abort and move to the next p-tuplet if the current region becomes empty after an intermediate intersection operation. The intersection of any region with an empty region is itself empty. Additionally, geometric criteria (i.e. non-overlapping bounding boxes) can be used to avoid performing unnecessary intersection operations.

IMPLEMENTATION & VALIDATION

The numerical models discussed in the previous section are implemented in both MATLAB and C++. The polygon clipping library GPC[11,12] is written in C and is directly integrated in a C++ environment, and indirectly in MATLAB via a MEX interface. Extensive documentation of both implementations may be found in the thesis produced during this study.[13] Fixed multiplicity models (i.e. single, double, triple, quadruple) are implemented in a straightforward way using nested loops.

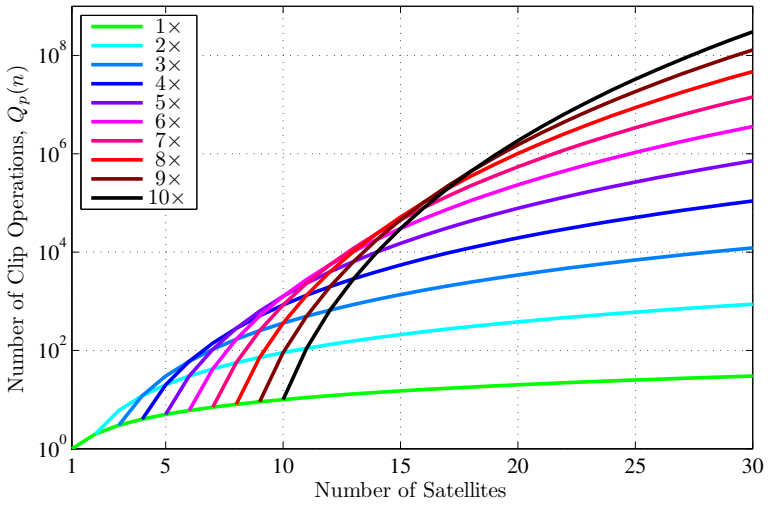

Figure 8: Clip Operations, $Q_p(n)$ vs. Number of Satellites

Combinations of satellite coverage regions are iterated through by the loop variables while performing the necessary Boolean operations to determine coverage regions of the specified multiplicity. A special approach is necessary for the arbitrary multiplicity case. A loop structure generates indices denoting the $q_p(n) \equiv \binom{n}{p}$ combinations of satellites for analysis during execution, avoiding the need for prior knowledge of coverage multiplicity prior to runtime.

For validation, the analytical model presented by Marchand and Kobel[4] is employed for the examples presented here. This model considers a single omni-directional sensor platform, in a circular orbit, covering a dual-altitude band target region. Additional validation and analyses on approximation error are presented in earlier publications[13] produced during the course of this study. An initial polygon resolution of 100 points per contour is found to be sufficient to achieve relative error below 0.1% compared to the analytical formulation.

APPLICATION

Time-Invariant Problems

Cases where the distances between the satellites and target regions remain fixed may be considered time-invariant. That is, the amount of ATH coverage remains constant as the satellites in the constellation evolve along their orbit. Based on this assumption, the following examples demonstrate the use of the proposed methodology in optimal constellation design. The first example presents the minimum number of satellites required, over a range of constellation altitudes, to achieve 99.9% single, double, and triple coverage over a range of altitudes. The second example expands on this by also considering the sensor range as a design parameter.

Example 1: A Single Independent Variable Case A planar constellation providing ATH coverage to an Earth-centered annular target region is considered. The n omni-directional sensor platforms are equally distributed in a single circular orbit. Constellation altitudes between 100 and 6000 km are considered at 1 km resolution. At each altitude, the minimum constellation populations providing at least 99.9% single, double, or triple coverage are determined with a simple grid search, the

results of which are shown in Figure 9. Just as coverage area is computed numerically, so is the area of the target region. Due to roundoff and truncation error, the two computed areas may not be the same, despite representing the exact same regions. To prevent this from causing an erroneous result, 99.9% coverage is considered rather than 100%. The minimum-altitude constellation configurations providing single, double, and triple coverage are shown in Figures 10a-10c.

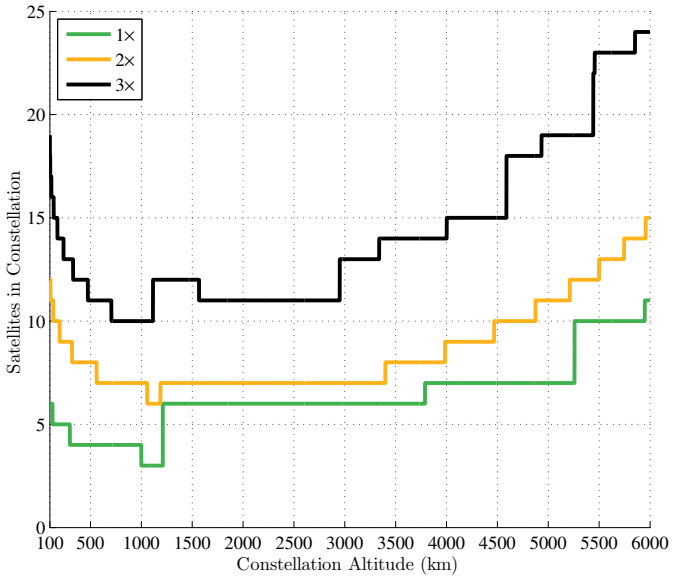

Figure 9: Minimum Constellation Population vs. Altitude

Table 1: Example 1 Parameters

Parameter	Description	Value
h_t	tangent height	100 km
h_l	lower target altitude	1000 km
h_u	upper target altitude	5000 km
R	omni-directional sensor range	10000 km
m	initial polygon resolution	100 PPC

Table 2: Example 1 Optimal Solutions

Coverage Mult.	Optimal Pop.	Altitude Range
$1\times$	3 satellites	$999 - 1210$ km
$2\times$	6 satellites	$1058 - 1187$ km
$3\times$	10 satellites	$705 - 1113$ km

Example 2: A Two Independent Variable Case Expanding upon the problem in Example 1, in addition to varying circular orbit altitude (19500-36000 km), variation in omni-directional sen-

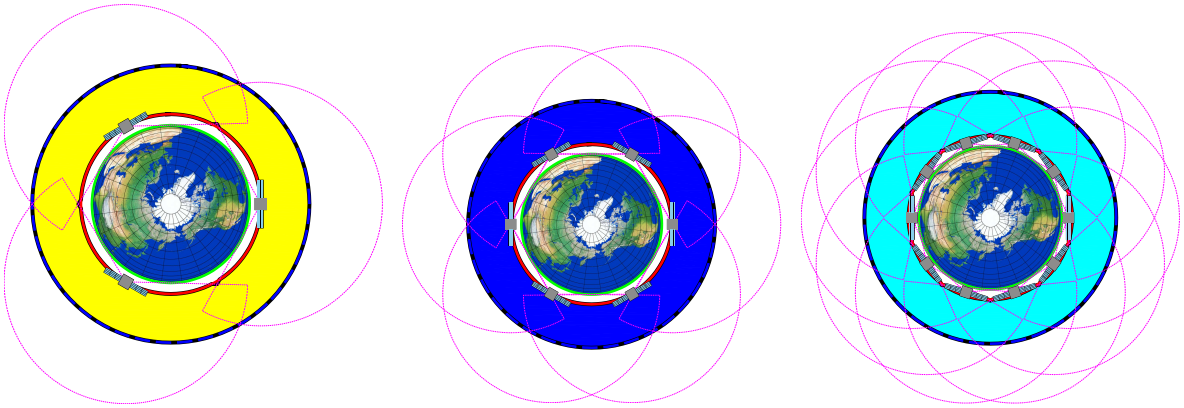

(a) $1\times$ cov., 3 sat., $h = 999$ km (b) $2\times$ cov., 6 sat., $h = 1058$ km (c) $3\times$ cov., 10 sat., $h = 705$ km

Figure 10: Smallest Constellations Providing at Least 99.9% ATH Coverage at Different Multiplicities

sor range (17000-30000 km) is considered in a 400×400 grid. Typically, sensor range is a fixed quantity depending upon available hardware. However, such an analysis may be useful during a trade study to determine the minimum sensor performance required to achieve coverage subject to other constraints. The problem parameters are shown in Table 3. The minimum number of satellites required to achieve at least 99.9% single coverage across the phase space is shown in Figure 11.

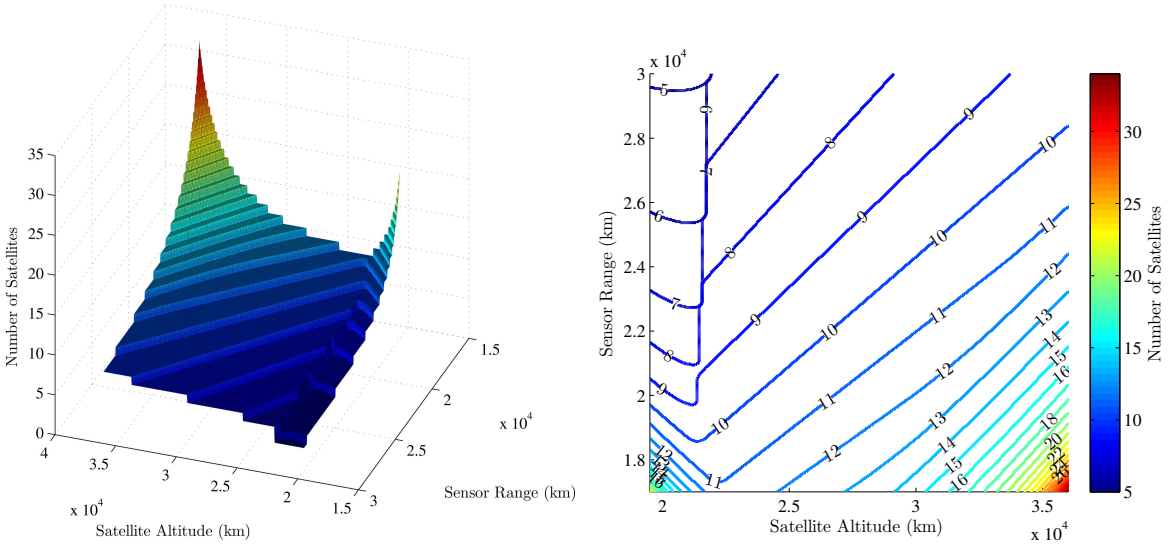

(a) (b)

Figure 11: Minimum Constellation Size For 99.9% Single Coverage vs. Altitude and Sensor Range

Time-Varying Problems

In cases with elliptical orbits, more complex target regions, or even constellations with populations distributed across multiple circular and/or elliptical orbits (in the same plane), the ATH

Table 3: Example 2 Parameters

Parameter	Description	Value
h_t	tangent height	100 km
h_l	lower target altitude	20000 km
h_u	upper target altitude	36000 km
m	initial polygon resolution	100 PPC

coverage amount is time-varying in general. The overlap between sensor coverage and target regions varies continuously.

Time-varying problems may be analyzed using the techniques developed in this study by performing instantaneous coverage evaluations at specified times throughout a time interval of interest. Figure 12 shows the ATH coverage provided by a planar constellation of 6 sensor platforms in arbitrarily prescribed orbits with arbitrarily defined sensor profiles over a prescribed time interval. A sufficiently long time interval, and a sufficiently short time-step must be selected to ensure the analysis adequately characterizes the behavior of the system. In a system with periodic behavior, an appropriate time interval is one period. However, non-periodic cases such as that shown in Figure 12 are more difficult to analyze because the judgment of the analyst must dictate an appropriate time interval.

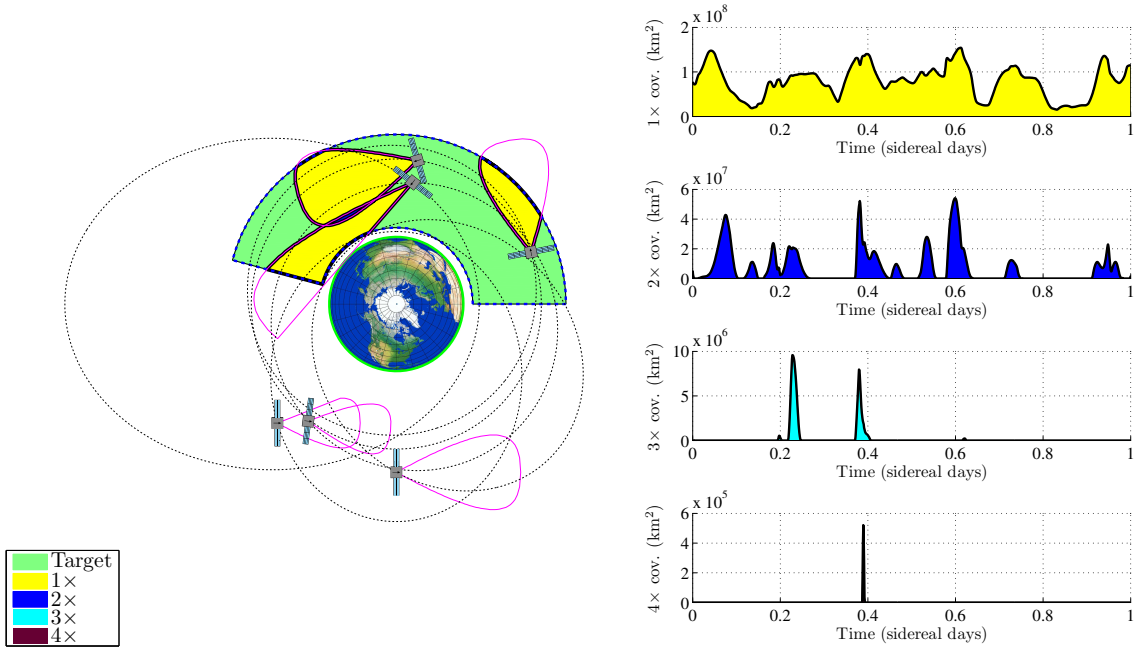

Figure 12: ATH Coverage Over Time – Arbitrary Sensor Profiles, Asymmetric Target Region

Using this numerical approach, constellation design problems can be addressed using various parameter optimization techniques.

Example 3: Analysis of Coverage by Elliptical Orbits As in the time-invariant problems, an annular target region is considered. However, due to the time-invariant nature of the target region itself, a time-invariant solution is optimal, as is demonstrated in this example.

The problem is posed as a Mixed-Integer Non-Linear Programming (MINLP) problem and solved using MIDACO.[16] MIDACO is a zeroth order heuristic solver and uses an ant colony optimization (ACO) approach.[17] Because ACO is a heuristic approach to MINLP, there are no analytical optimality criteria for non-convex problems such as this, thus the algorithm is allowed to run until it ceases improvement upon the solution.

A constellation composed of two elliptical orbits with opposite periapsis directions is considered. Each orbit is initially populated by three satellites, each group with dissimilar omni-directional sensor performance. Within each orbit the satellites are equally spaced in mean anomaly. The objective is the minimize the total population of the constellation, while ensuring continuous single coverage of the target region. The formulation allows for one or both orbits to have zero population (although zero population in both orbits results in an obvious violation of the continuous coverage constraint). Problem parameters are summarized in Table 4.

Table 4: Example 3 Parameters

Parameter	Description	Value
h_t	tangent height	100 km
h_l	lower target altitude	1000 km
h_u	upper target altitude	10000 km
k	number of distinct orbits in constellation	2 orbits
R_1	omni-directional sensor range of sats. in orbit 1	5000 km
R_2	omni-directional sensor range of sats. in orbit 2	10000 km
m	initial polygon resolution	100 PPC

Table 5: Example 3 Start Point & Solution (682 func. evals, 300s)

Decision Variable	Description	Start Point	Solution
a	semi-major axis (both orbits)	10000 km	8588.0
e	eccentricity (both orbits)	0.25	0
M_{2_0}	M at epoch for lead sat. in orbit 2	0 rad	0 rad
n_1	orbit 1 population	3 satellites	0 satellites
n_2	orbit 2 population	3 satellites	6 satellites

Table 5 shows the start point and solution after 300 seconds (682 function evaluations). From an infeasible start point (coverage gaps), a feasible 12 satellite state is identified by the 15th function evaluation. By the 98th function evaluation, the presented solution is converged upon. With 6 satellites distributed in a single circular orbit, the solution is time-invariant when only concerned with the quantity of coverage, as expected.

Example 4: Continuous Observation of CONUS GEO Satellites In contrast to the previous example, an asymmetric Earth-fixed target region is considered here. From a geostationary orbit,

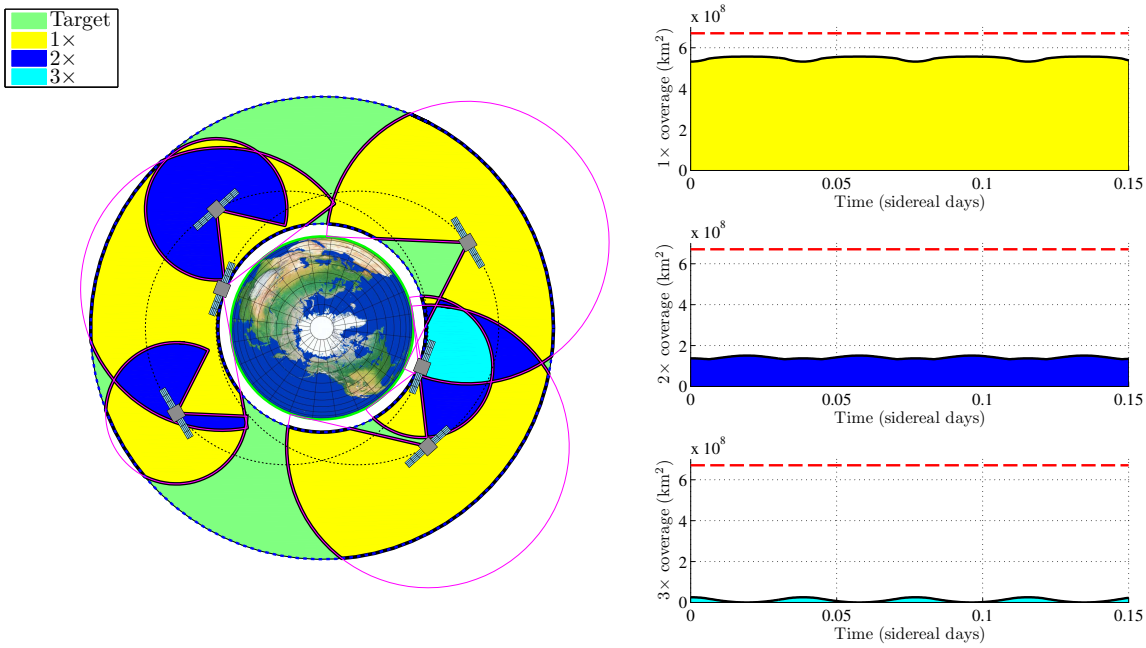

(a) Start Point

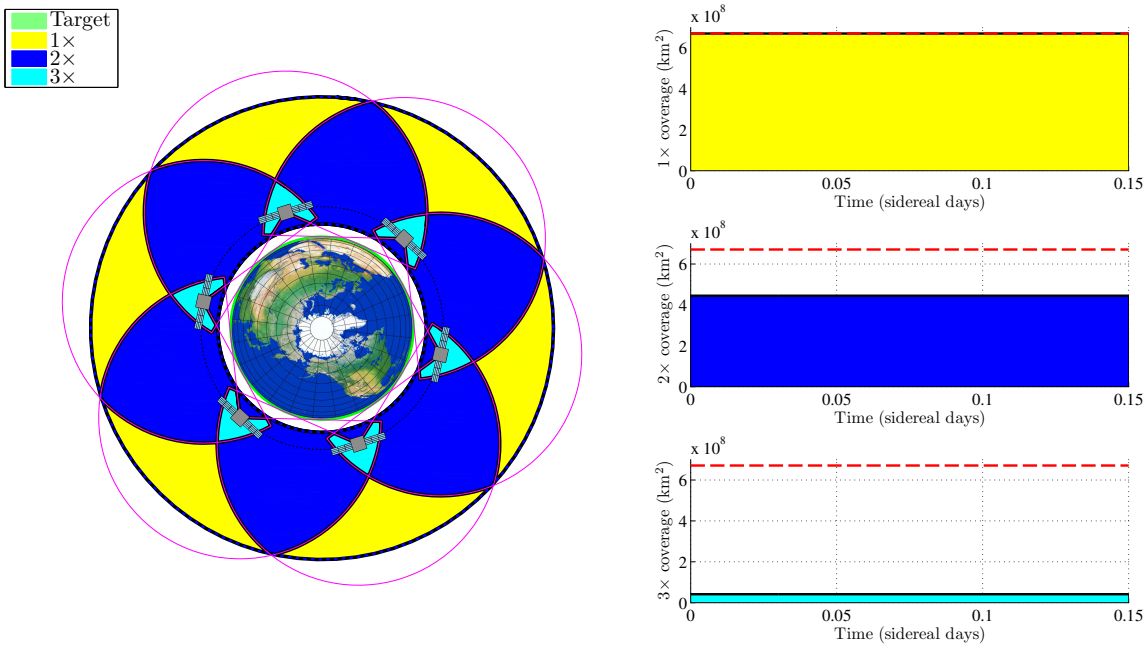

(b) Solution

Figure 13: Start Point to Solution With Continuous 1× Coverage Constraint

the target region is defined as ± 1000 km in altitude, between 148°W and 61°W longitude (populated by satellites serving the continental United States).

One immediately obvious solution corresponds to placing the satellites on a geostationary orbit. However, because this particular arrangement is itself time-invariant, it is not particularly useful in demonstrating the algorithm's capability for addressing time-varying problems. Instead, consider an alternate arrangement where the constellation is composed of satellites placed across four smaller identical orbits, equally distributed in periapsis direction. Unlike previous examples, the satellites are no longer equally distributed within each orbit, and are instead equally distributed within a range in mean anomaly. The positioning (mean anomaly at epoch) of each group is prescribed such that apoapsis of the center of each satellite group occurs as the target region is centered above apoapsis of each orbit. In order to maintain this synchronization, the time period (and thus semi-major axis) of the orbits is prescribed to revisit geostationary altitude an integer number of times per day (twice daily in this example).

The objective in this example is to minimize the satellite sensor range, i.e. determine the smallest sensor range capable of covering the target region continuously. The problem is subsequently posed as a non-linear programming (NLP) problem, where all integer parameters are prescribed, and approached using the interior-point solver in *fmincon*.[18] The decision variables are satellite sensor range, R, orbit eccentricity e, and satellite group spread, ΔM. Problem parameters are summarized in Table 6.

Table 6: Example 4 Parameters

Parameter	Description	Value
h_t	tangent height	100 km
h_l	lower target altitude	41164.13 km
h_u	upper target altitude	43164.13 km
λ_l	western target longitude	148°W
λ_u	eastern target longitude	61°W
k	number of distinct orbits in constellation	4 orbits
n	total constellation population	8 satellites
m	initial polygon resolution	100 PPC

Table 7: Example 4 Start Point & Solution

Decision Variable	Description	Start Point	Solution
R	omni-directional sensor range	12000 km	17444 km
e	orbit eccentricity	0.50	0.40
ΔM	group spread	90° km	89.4°

Table 7 shows the infeasible start point and solution, obtained after 32 iterations. The start point and solution constellations are shown in Figures 14a and 14b respectively. Although the number of satellites in each orbit and the constellation as a whole remain fixed, this example demonstrates how the numerical ATH coverage model may be used in an NLP-driven constellation design process.

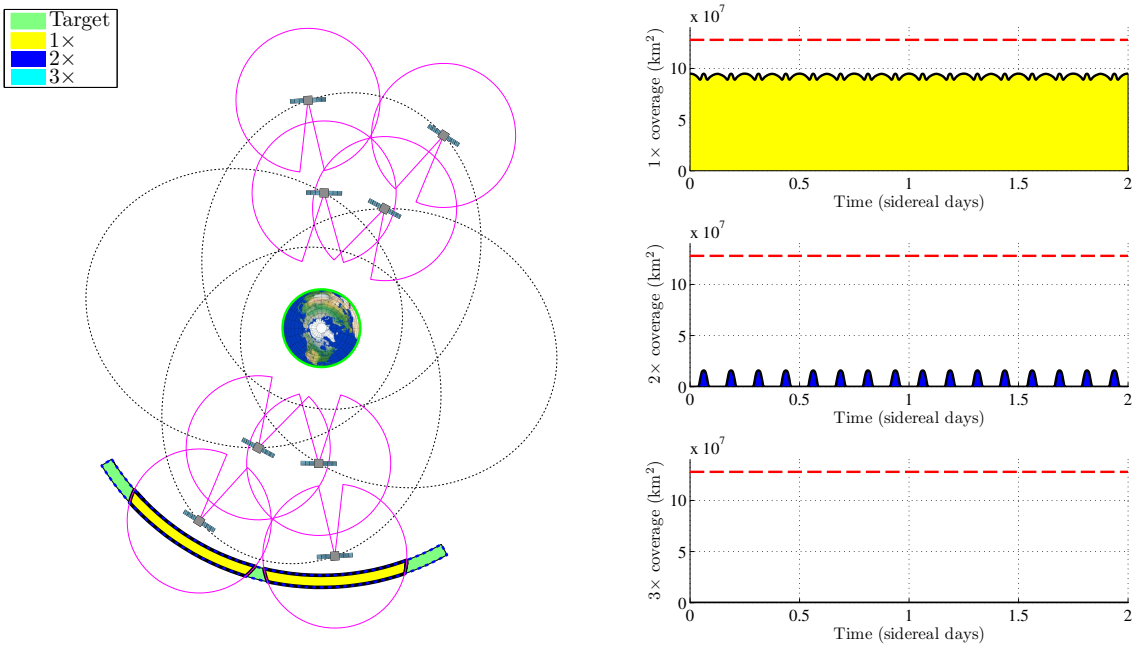

(a) Start Point

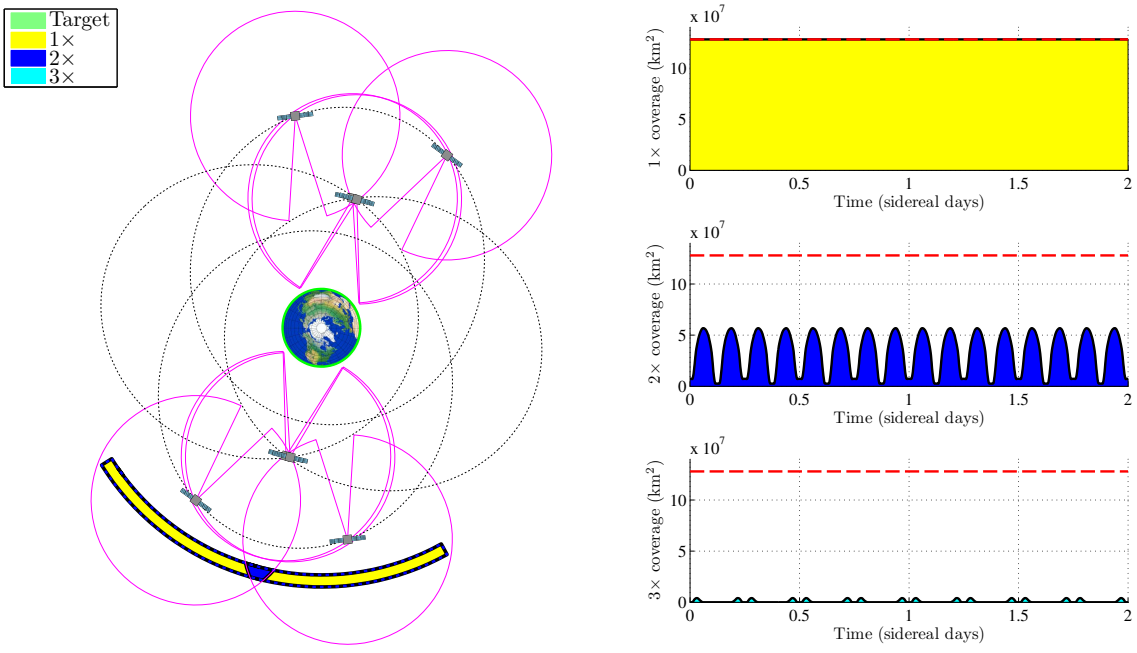

(b) Solution

Figure 14: Start Point to Solution With Continuous 1× Coverage Constraint

CONCLUSION

An efficient numerical algorithm is devised, based on concepts from computer graphics, that facilitates the optimal constellation design for space-based space situational awareness applications. The proposed approach is effective and efficient in addressing both time-invariant and time-varying problems and further addresses n-tuple coverage from a numerical perspective. The results presented in this study also demonstrate the success of this approach in addressing the complexities of heterogeneous sensor and orbital configurations within the constellation. This is of particular importance because exact representations of above the horizon coverage are not available in such cases.

ACKNOWLEDGMENTS

This research was carried out at The University of Texas at Austin and was funded by the Air Force Office of Scientific Research through the Air Force Young Investigator Award, contract # FA9550-09-1-0227. Any opinions, findings, and conclusions or recommendations expressed in this material are those of the authors and do not necessarily reflect the views of the funding agency.

REFERENCES

[1] L. Rider and W. S. Adams, "Circular Polar Constellations Providing Continuous Single or Multiple Coverage Above a Specified Latitude," *Journal of the Astronautical Sciences*, Vol. 35, 1987, pp. 155–192.

[2] J. G. Walker, "Circular Orbit Patterns Providing Continuous Whole Earth Coverage," Tech. Rep. 70211, Royal Aircraft Establishment, November 1970.

[3] J. G. Walker, "Continuous Whole Earth Coverage by Circular Orbit Satellite Patterns," Tech. Rep. 77044, Royal Aircraft Establishment, March 1977.

[4] B. G. Marchand and C. Kobel, "Geometry of Optimal Coverage for Space Based Targets with Visibility Constraints," *The Journal of Spacecraft and Rockets*, Vol. 46, No. 4, 2009, pp. 845–857.

[5] L. Rider, "Optimal orbital constellations for global viewing of targets against a space background," *Optical Engineering*, Vol. 19, No. 2, 1980, pp. 219–223.

[6] L. Rider, "Design of low to medium altitude surveillance systems providing continuous multiple above-the-horizon viewing," *Optical Engineering*, Vol. 28, No. 1, 1989, pp. 25–29.

[7] K. J. Gordon, "The Computation of Satellite Constellation Range Characteristics," *AIAA/AAS Astrodynamics Conference*, August 1994, pp. 1–9.

[8] D. C. Beste, "Design of Satellite Constellations for Optimal Continuous Coverage," *IEEE Transactions on Aerospace and Electronic Systems*, Vol. 14, No. 3, 1978, pp. 466–473.

[9] J. M. Hanson and A. N. Linden, "Improved Low-Altitude Constellation Design Methods," *Journal of Guidance, Control, and Dynamics*, Vol. 12, No. 2, 1988, pp. 228–236.

[10] M. d. Berg, O. Cheong, M. v. Kreveld, and M. Overmars, *Computational Geometry: Algorithms and Applications*. Springer-Verlag, 3 ed., 2008.

[11] A. Murta, “General Polygon Clipping Library,” http://www.cs.man.ac.uk/~toby/alan/software/.

[12] B. Vatti, “A Generic Solution to Polygon Clipping,” *Communications of the ACM*, Vol. 35, No. 7, 1992, pp. 57–63.

[13] A. T. Takano, “Numerical Analysis and Design of Satellite Constellations for Above the Horizon Coverage,” Master’s thesis, The University of Texas at Austin, 2010.

[14] W. H. Beyer, ed., *CRC Standard Mathematical Tables*, pp. 123–124. CRC Press, 28 ed., 1987.

[15] J. H. Conway and R. K. Guy, *The Book of Numbers*, ch. 3, pp. 67–68. Springer-Verlag, 1 ed., 1996.

[16] M. Schlueter, J. J. Rckmann, and M. Gerdts, “Mixed Integer Distributed Ant Colony Optimization,” http://www.midaco-solver.com/index.html.

[17] M. Schlueter, J. A. Egea, and J. R. Banga, “Extended ant colony optimization for non-convex mixed integer nonlinear programming,” *Computers and Operations Research*, Vol. 36, No. 7, 2009, pp. 2217–2229.

[18] The MathWorks, *Fmincon*. http://www.mathworks.com/help/toolbox/optim/ug/fmincon.html.